Progress In Electromagnetics Research M, Vol. 6, 167–184, 2009

THEORETICAL MODELING OF A METAL-CLAD PLANAR WAVEGUIDE BASED BIOSENSORS FOR THE DETECTION OF PSEUDOMONAS-LIKE BACTERIA

V. Singh and D. Kumar

Department of Physics
Banaras Hindu University
Varanasi, U. P., India

Abstract—In this paper, a metal-clad planar optical waveguide biosensor with five layer structure is studied theoretically for the detection of Pseudomonas and Pseudomonas-like bacteria. Using a very simple boundary matching technique, we derive the mode equation and other necessary formulae for the proposed biosensor and analyse its performance under different conditions related to its constituents. The numerical results presented in this paper leads to a significant optimization of the important design parameters to sense micro-scale biological objects. Also, we compare our computed results with the results given for a biosensor with four layer structure. In addition, we discuss the importance and need of the inclusion of the thickness of an affinity layer as fifth layer in the four layer structure of the metal clad planar waveguide.

1. INTRODUCTION

A biosensor is a self contained integrated device which can provide specific and quantitative analytical information about the presence or the concentration of biological molecules, structures and microorganism ranging in size from nanometers to micrometers such as DNA, proteins, lipid bilayers, bacteria and whole cell behaviour. In a classic paper [1], Tiefenthaler and Lukosz introduced for the first time, a planar optical waveguide for sensing gas and humidity by measuring a change in the refractive index (RI) of the material contained in the cover of waveguide. Thereafter, tremendous advances in optical waveguide sensors have taken place for humidity sensing, heavy metal

Corresponding author: V. Singh (dr_vivek_singh@indiatimes.com).

ions sensing, chemical sensing, biochemical sensing and biosensing [2–6]. The tremendous international interest in optical sensors can be seen from the very large number of research, technical and review articles published in several international journals of repute [7–9, 31–33]. Optical fiber based biosensors have been the focus of a large volume of research in the past few years. Enzyme optical fiber based biosensors continue to be the most commonly reported type [10]. However, the number of publications on immunoassay, nucleic acid and whole cell optical fiber based biosensors has greatly increased [9–11]. Presently Surface Plasmon Resonance (SPR) sensor technology has been commercialized, and SPR biosensors have become a central tool for characterizing and quantifying bimolecular interactions [12, 13]. The optical waveguide sensor is also known as evanescent wave sensor because of the evanescent wave entering into the cover medium whose RI is to be measured. But the probing depth of the evanescent field has an upper limit of 100–150 nm. Therefore, such sensors can only detect biological substances in the close vicinity to the sensor surface limited to below 200 nm. But for whole-cell behaviour and micron sized biological objects, the probing depth of the evanescent field must be increased. Recently Horwath et al. [14] have shown that probing depth can be increased much using reverse symmetry configuration for detecting whole-cell behaviour and micron sized biological objects.

Very recently metal clad optical waveguide sensors have been applied to detect biological objects of micrometer size [15, 16]. Significant attempts have been made towards the development of evanescent field (EF) sensor for biological sensing which are based on the interaction of evanescent field of a planar waveguide mode with the surrounding media and the resulting perturbation of waveguide mode effective index [17–19]. Using the thin high contrast index material such as silicon-on-insulation (SIO) photonic wire based technique, Densmore et al. [20] have shown that simple SOI-wire-waveguide based EF sensors can provide a higher sensitivity to surface adsorption and bulk homogeneous index change than planar waveguide sensor because such high index contrast waveguides give large and strongly localized electric field distribution with penetration depth much larger than the 200 nm needed for better biological sensing [14]. Despite these advances [21–25] much more work needs to be done before optical fiber based-biosensors become commercially viable option for sensing. Moreover the attachment of marine Pseudomonas sp. to a variety of surface was investigated and it was found that these bacteria are attached not only on special carbon sources (nicotine, toluene, octane etc.) but also on some hydrophobic plastic [Teflon, polyethylene, polystyrene, poly(ethylene terephthalate)] with little or

no surface charge [26–30].

In the present investigation, we report a theoretical analysis of a metal-clad planar waveguide based biosensor having five layers for the detection of Pseudomonas and Pseudomonas-like bacteria. Here we propose to take 1 mm thick glass plate as a substrate [n_S = 1.48534(FK51A)], a metal cladding of 30 nm silver ($n_M = 0.065 + i4.0$) or gold ($n_M = 0.15 + i3.2$), a 500 nm thick polystyrene (PS) film (n_F = 1.59); the affinity layer is approximately 30–60 nm thick and coated with carbon source or hydrophobic plastic. The necessary formulas are derived and given in appendix to study the performance of proposed biosensor under different conditions related to its constituents. The numerical results presented in this article are compared with those of metal clad planar waveguide biosensor having four layers [16]. Comparison leads to a significant optimization of the important design properties to sense micron-scale biological objects like Pseudomonas and Pseudomonas-like bacteria.

The present study is organized in the following way. Section 2 is the modeling section where description of the modeling is given in brief and related equations which are given in appendix in detail. Section 3 is concerned with the application of our formulation for a new structure for some chosen parameters. Here we examine the sensing features and the different behaviours of our proposed structure theoretically. Finally, in Section 4, conclusions are presented and it has been emphasized that dip type silver metal clad planar waveguide biosensor is more preferable for microbial detection. In this section, we will present several numerical results to demonstrate the need of the inclusion of the thickness of an affinity layer as the fifth layer in the four layer structure of the metal clad planar waveguide [15, 16].

2. THEORETICAL MODELING

A schematic configuration of the proposed waveguide is shown in Fig. 1. It consists of five layers of a substrate (S), a metal (M), a film (F), an affinity layer (A) and a cover (C). A thin metallic layer with permittivity ε_M, permeability μ_M, and thickness d_M is sandwiched between a semi-infinite substrate with permittivity ε_S, permeability μ_S, and a guiding layer with permittivity ε_F, permeability μ_F, and thickness d_F. The upper surface of the guiding layer is coated with organic material with permittivity ε_A, permeability μ_A, and affinity thickness d_A and covered by cladding with permittivity ε_C and permeability μ_C. Here we assume that all the materials are non-magnetic i.e., μ's = 1; also all the materials are lossless, i.e., ε's are real except the metallic region. In order to see the sensor performance

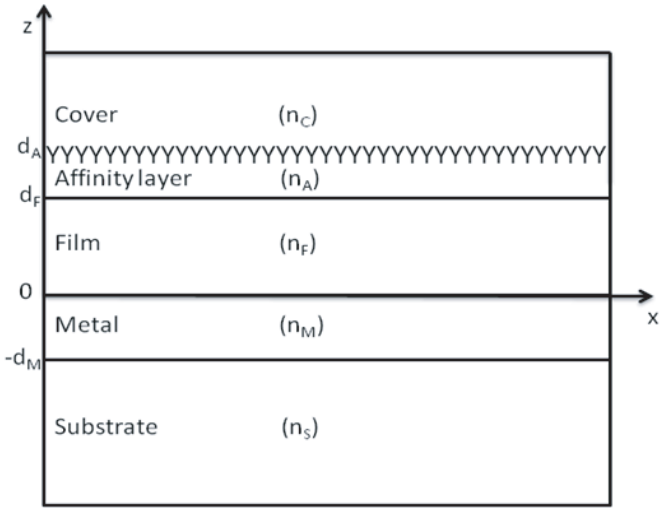

Figure 1. Schematic diagram of a five-layer waveguide with their refractive indices.

we solve Maxwell's equations for the five-layered structure and get the Helmholtz equations which are outlined in appendix in more details with their solutions.

Now applying the boundary conditions and considering that the fields and their first derivative should be continuous at the substrate-/metal, metal-film, film-affinity, affinity-cover media boundaries. As a result of this matching we get the following dispersion relation for the proposed five layered waveguide.

$$2\pi m = 2k_F d_F - \phi_{F,M,S} - \phi_{F,A,C} \tag{1}$$

where all the terms are defined in appendix.

Finally, by using some straightforward steps the reflectance of the proposed waveguide can be written as

$$R = |r_{S,M,F,A,C}|^2 = \left| \frac{r_{S,M} + r_{M,F,A,C}\ e^{2ik_M d_M}}{1 + r_{S,M} r_{M,F,A,C}\ e^{2ik_M d_M}} \right|^2 \tag{2}$$

all the terms are defined in appendix.

By matching the field at the boundaries we get a set of eight equations having eight unknown constants. These equations are written as

$$\Delta\psi = 0 \tag{3}$$

where Δ is 8×8 determinant having elements given in appendix.

$$\psi = (A_C,\, A_A,\, B_A,\, A_F,\, B_F,\, A_M,\, B_M,\, B_S);$$

The modal profile of a waveguide mode for a proposed waveguide structure with a given width and the corresponding effective refractive index and calculated from Eq. (3) can now be calculated from Eq. (5) by assuming one of the field amplitude $A_F = 1$. Moreover the sensitivity of the waveguide is the function of effective refractive index N, affinity refractive index n_A, film refractive index n_F, affinity thickness d_A and film thickness d_F.

$$S = S(N,\, n_A,\, n_F,\, d_A,\, d_F) \tag{4}$$

Hence affinity sensitivity with respect to affinity refractive index and affinity thickness are approximately defined as

$$\frac{dN}{dn_A} = \frac{\frac{\partial S}{\partial n_A}}{\frac{\partial S}{\partial N}} \tag{5}$$

$$\frac{dN}{d(d_A)} = \frac{\frac{\partial S}{\partial d_A}}{\frac{\partial S}{\partial N}} \tag{6}$$

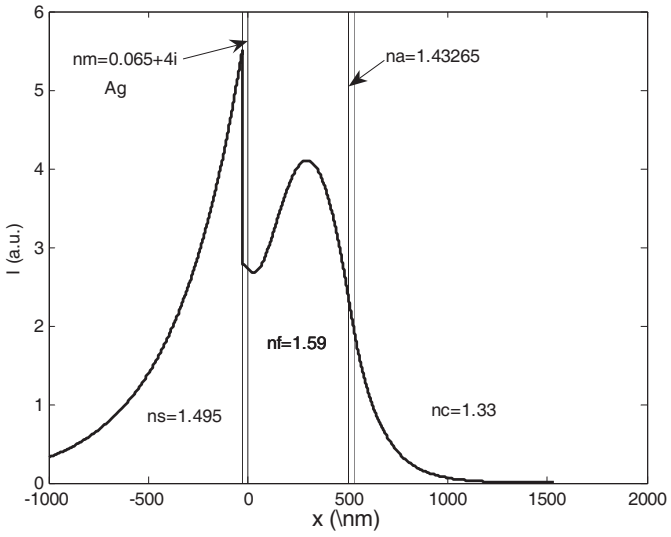

(a)

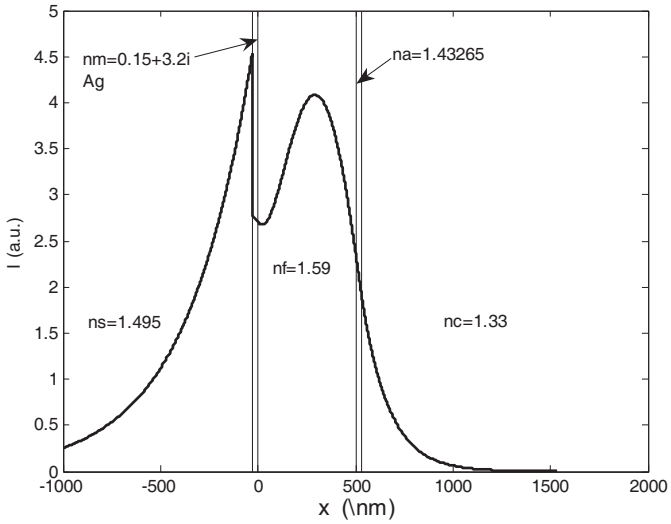

(b)

Figure 2. (a) Modal field distribution of a metal clad planar waveguide sensor with a silver cladding for TE component. (b) Modal field distribution of a metal clad planar waveguide sensor with a gold cladding for TE component.

3. NUMERICAL RESULTS AND DISCUSSION

We have chosen the following parameters: an operating wavelength $\lambda_0 = 0.6328\,\mu\text{m}$, the refractive indices of the substrate, metal, and film are $n_S = 1.495$, $n_M = 0.064 + 4i$ (silver), $n_M = 0.15 + 3.2i$ (gold), $n_F = 1.59$ respectively. The corresponding width of metal and film layers are $d_M = 0.03\,\mu\text{m}$, $d_F = 0.5\,\mu\text{m}$. Now we plot the modal field distribution of the proposed waveguide structure using a very simple approach as described above in Section 2. The field distribution obtained by this approach is shown in Fig. 2(a) and Fig. 2(b) for two different metal films of proposed waveguide structure for TE component. The field distributions are in expected shape. It is clear that in the silver metallic film the field is highly attenuated compared with the field obtained in the case of gold metallic film at substrate-metal surface. This indicates that the silver metallic film at substrate-metal surface provides a sharper reflectance dip than the gold metallic film. Therefore, silver-metallic film is preferable to resolve the small changes in RI (n_c) of cover medium. The sensor property of the proposed waveguide is optimized by achieving the largest change in

the reflectance of the waveguide. Hence we compute the values of reflectance reflectance R using Eq. (2) for various values of incident angle θ_I and we plot the curves between R and θ_I as illustrated in Fig. 3 and Fig. 4.

It is clear from Fig. 3 and Fig. 4 that as the cover refractive index changes from $n_C = 1.33$ to $n_C = 1.35$ the dip of reflectance shifts towards higher value of θ_1. This will be the signature of bacteria and the shift in the angle θ_1 is totally dependent on the concentration and

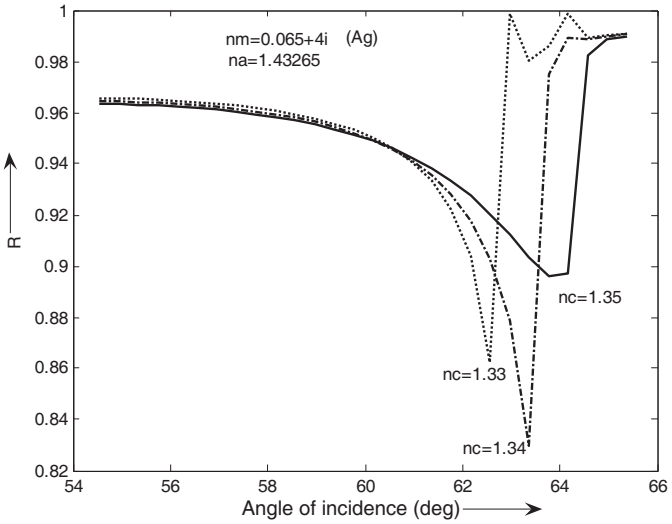

(a)

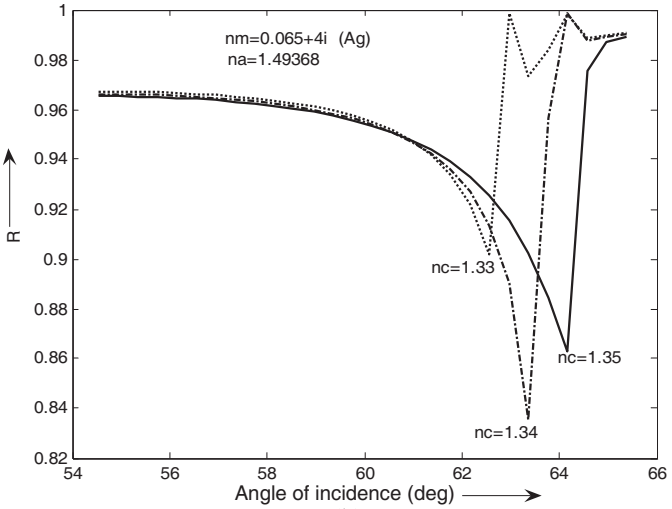

(b)

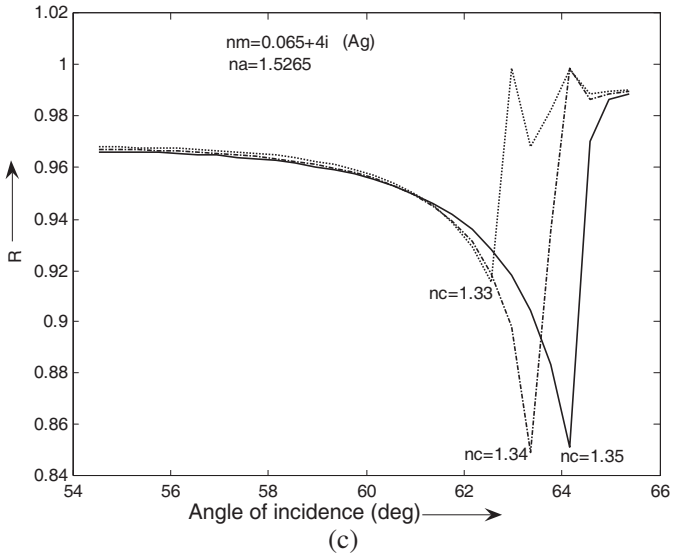

(c)

Figure 3. (a) Calculated Fresnell reflectance for TE polarized light for proposed waveguide with silver cladding. The refractive indices and thickness used are: $n_S = 1.49$, $n_F = 1.59$, $d_M = 0.03\,\mu\text{m}$, $d_F = 0.5\,\mu\text{m}$, $d_A = 0.06\,\mu\text{m}$. (b) Calculated Fresnell reflectance for TE polarized light for proposed waveguide with silver cladding. The refractive indices and thickness used are: $n_S = 1.49$, $n_F = 1.59$, $d_M = 0.03\,\mu\text{m}$, $d_F = 0.5\,\mu\text{m}$, $d_A = 0.045\,\mu\text{m}$. (c) Calculated Fresnell reflectance for TE polarized light for proposed waveguide with silver cladding. The refractive indices and thickness used are: $n_S = 1.49$, $n_F = 1.59$, $d_M = 0.03\,\mu\text{m}$, $d_F = 0.5\,\mu\text{m}$, $d_A = 0.04\,\mu\text{m}$.

mobility of bacteria. The attachment of bacteria to affinity surfaces is an important phenomenon in this waveguide. When the bacteria is attached on the affinity surface then refractive index of cover medium changes, and this change of refractive index is dependent on the culture concentration of the bacteria and their mobility. In Fig. 3, the three different affinity layers for the detection of Pseudomonas having refractive indices 1.4370 [poly(trifluoroethyl methacrylate)], 1.49268 (toluene) and 1.5265 (nicotine) are selected. It is clear from Fig. 3(a) that for [poly(trifluoroethyl methacrylate)] material the small change in n_c, for $n_c = 1.33$ to $n_c = 1.34$ the dip is sharp but for $n_c = 1.35$ the dip is blunt. Here under the same condition [see Fig. 3(b) and Fig. 3(c)] the toluene and nicotine will give better result than poly(trifluoroethyl methacrylate). If we compare the result obtained for Fig. 3 (silver) with

Fig. 4 (gold) then in all the three cases the dip is blunt at $n_c = 1.35$ for gold and have tendency to become sharp for higher refractive index materials for both metallic films. In this way we can say that the silver coating substrate-metal surface will give better information than gold coating. Here we also conclude that if the refractive index of affinity layer ($n_A = 1.5265$) is large then the dip is sharp and we get more reliable information regarding the detection of Pseudomonas and

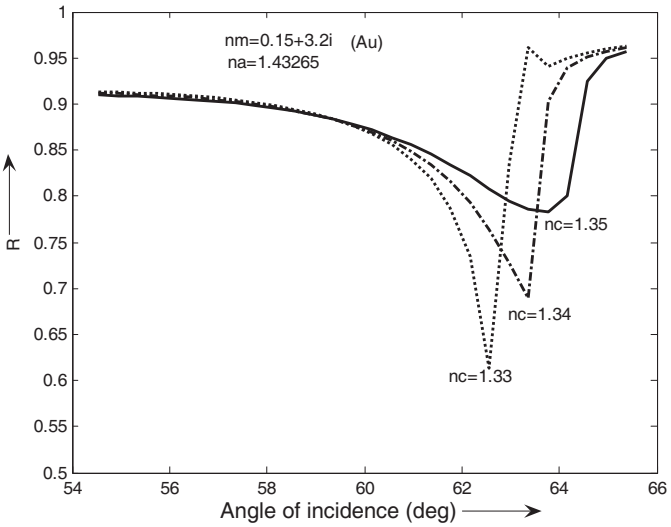

(a)

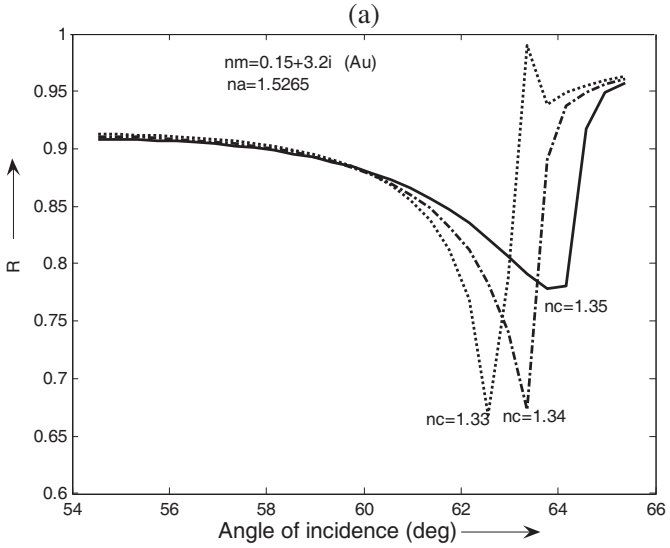

(b)

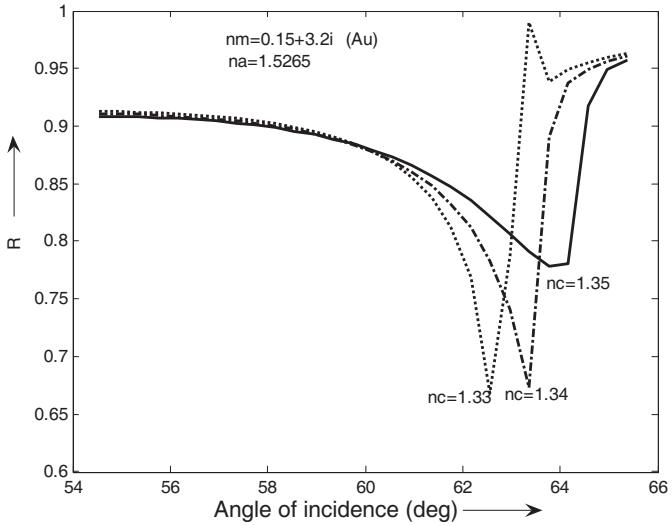

(c)

Figure 4. (a) Calculated Fresnell reflectance for TE polarized light for proposed waveguide with gold cladding. The refractive indices and thickness used are: $n_S = 1.49$, $n_F = 1.59$, $d_M = 0.3\,\mu\text{m}$, $d_F = 0.45\,\mu\text{m}$, $d_A = 0.025\,\mu\text{m}$. (b) Calculated Fresnell reflectance for TE polarized light for proposed waveguide with gold cladding. The refractive indices and thickness used are: $n_S = 1.49$, $n_F = 1.59$, $d_M = 0.3\,\mu\text{m}$, $d_F = 0.45\,\mu\text{m}$, $d_A = 0.05\,\mu\text{m}$. (c) Calculated Fresnell reflectance for TE polarized light for proposed waveguide with gold cladding. The refractive indices and thickness used are: $n_S = 1.49$, $n_F = 1.59$, $d_M = 0.3\,\mu\text{m}$, $d_F = 0.45\,\mu\text{m}$, $d_A = 0.03\,\mu\text{m}$.

other bacteria.

The variation of sensitivity to refractive index changes $\frac{\partial N}{\partial n_A}$, in the affinity layer with affinity thickness d_A for above three chosen materials is given in Fig. 5 (silver) and Fig. 7 (gold). In both cases we find the higher sensitivity for nicotine whose refractive index is higher than that of toluene and poly(trifluoroethyl methacrylate). The variation of sensitivity to thickness changes $\frac{\partial N}{\partial d_A}$, in the affinity layer with affinity thickness d_A for above three chosen materials is also shown in Fig. 6 (silver) and Fig. 8 (gold). Here the sensitivity of poly(trifluoroethyl methacrylate) for the silver coated substrate-metal surface is larger than toluene and nicotine upto $d_A = 85\,\text{nm}$ and after this the sensitivity of poly(trifluoroethyl methacrylate) decreases rapidly than those of toluene and nicotine in Fig. 6. Similar behavior

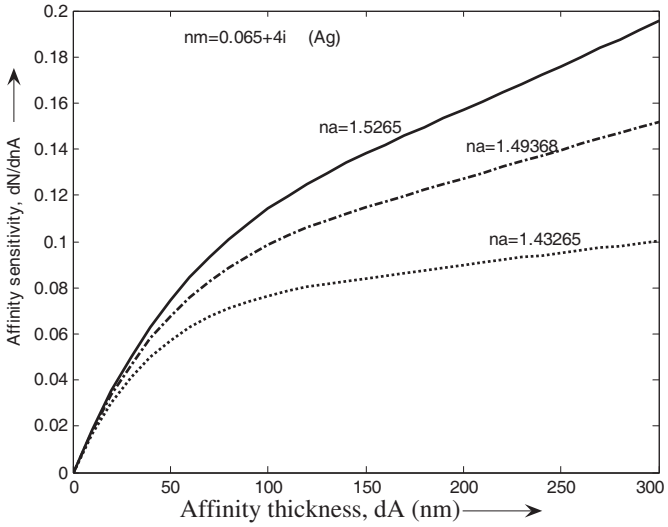

Figure 5. Sensitivity to refractive index changes $\frac{\partial N}{\partial n_A}$, in the affinity layer with affinity thickness d_A for silver coated waveguide.

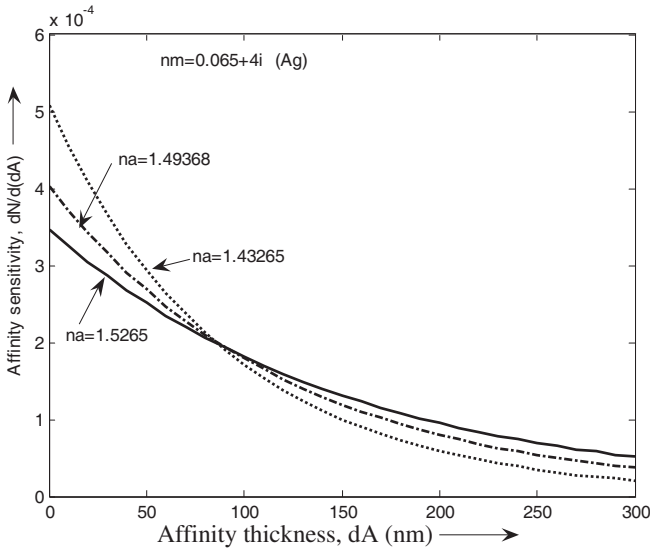

Figure 6. Sensitivity to thickness changes $\frac{\partial N}{\partial d_A}$, in the affinity layer with affinity thickness d_A for silver coated waveguide.

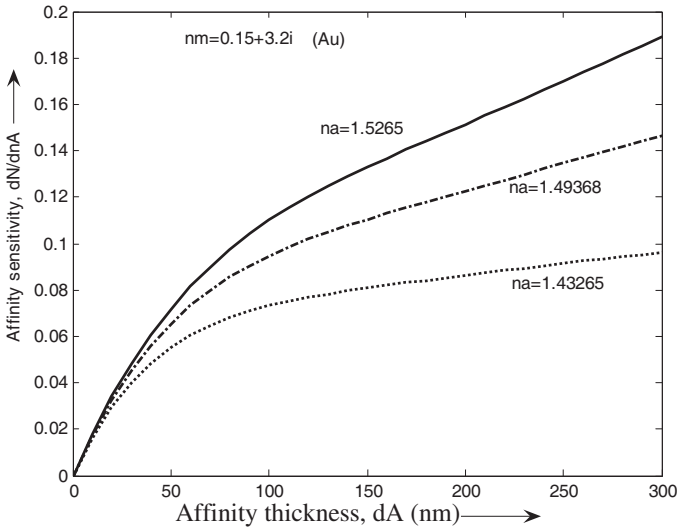

Figure 7. Sensitivity to refractive index changes $\frac{\partial N}{\partial n_A}$, in the affinity layer with affinity thickness d_A for gold coated waveguide.

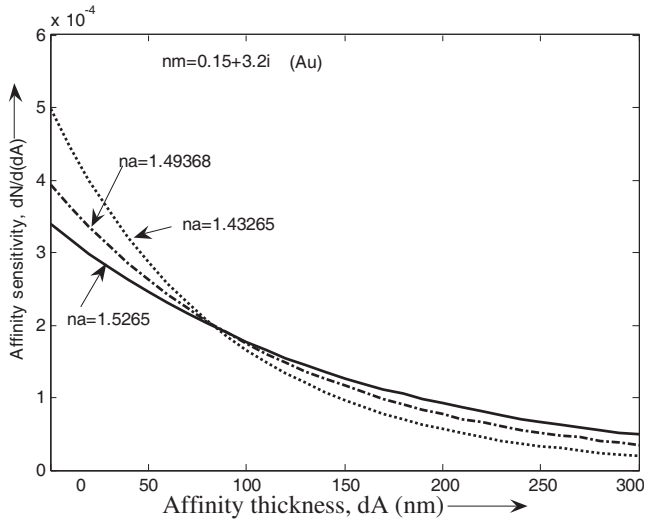

Figure 8. Sensitivity to thickness changes $\frac{\partial N}{\partial d_A}$, in the affinity layer with affinity thickness d_A for gold coated waveguide.

is also found in the case of gold coated substrate-metal surface in Fig. 7. Such type of behaviour is not given in [16]. Again, the variation of sensitivity to thickness changes $\frac{\partial N}{\partial d_A}$, in the affinity layer with affinity thickness d_A for nicotine is smaller than both toluene and poly(trifluoroethyl methacrylate). Now we are in a position to compare our computed results with the results given for four layer structure. Considering Fig. 5 and Fig. 7 it is clear that in our case the sensitivity due to $\frac{\partial N}{\partial n_A}$ against d_A is less than 0.2 where as in the case of four layer structure it is greater than 0.5. But when we examine Fig. 6 and Fig. 8 we note that in our case the sensitivity due to $\frac{\partial N}{\partial d_A}$ against d_A is nearly equal to 5.0×10^{-4} nm where as it is 3.0×10^{-4} nm for the four layer structure. Thus we find that the sensitivity due to $\frac{\partial N}{\partial n_A}$ is smaller in our case but at the same time the sensitivity due to $\frac{\partial N}{\partial d_A}$ is greater. Hence for greater sensitivity, the sensitivity due to $\frac{\partial N}{\partial d_A}$ against d_A is preferable for the proposed structure.

4. CONCLUSION

We have compared silver coated metal-clad waveguide biosensor with the gold coated metal-clad waveguide biosensor having some selected affinity layers for the detection of Pseudomonas and Pseudomonas-like bacteria. The following facts are finally concluded

1) The silver coated waveguide always gives better result than the gold coated one.
2) The affinity layer refractive index should be quite high for sharp dip (as in the case of nicotine which refractive index is higher than poly (trifluoroethyl methacrylate) and toluene).
3) For higher sensitivity the refractive index of affinity layer should be higher while the thickness of affinity layers should be smaller.
4) The choice of affinity layer as the fifth layer in our formulation seems more reasonable and convenient compared to the formation of adlayer during the process.

ACKNOWLEDGMENT

This work is supported by the Department of Science and Technology, DST New Delhi, under the fast track young scientist scheme No. SR/FTP/PS-42/2006. We are also thankful to Dr. R. D. S. Yadava and Dr. B. Prasad for their various supports and discussions.

APPENDIX A.

In order to see the performance of proposed biosensor we solve Maxwell's equations for five layer structure and get the Helmholtz equations which can be written as

$$\frac{\partial^2\psi(z)}{\partial z^2} + \left[\omega^2\varepsilon(z)\mu(z) - \beta^2\right]\psi(z) = 0 \tag{A1}$$

where ψ represents the electric field for TE-polarized light and the magnetic field for TM-polarized light; ω is the angular frequency of the field and β is the propagation constant in x-direction, which can be written as $\beta = k_0 N$, where k_0 is the free space wavenumber, and N is the modal effective index.

Hence the solutions of the proposed waveguide for different regions can be written as

$$\psi(z)=\begin{Bmatrix} A_C\exp(-ik_C z)e^{i(\omega t-k_x x)} & \text{Cover region} \\ \{A_A\exp(ik_A z)+B_A\exp(-ik_A z)\}\,e^{i(\omega t-k_x x)} & \text{Affinity region} \\ \{A_F\exp(ik_F z)+B_F\exp(-ik_F z)\}\,e^{i(\omega t-k_x x)} & \text{Film region} \\ \{A_M\exp(ik_M z)+B_M\exp(-ik_M z)\}\,e^{i(\omega t-k_x x)} & \text{Metal region} \\ A_S\exp(ik_S z)e^{i(\omega t-k_x x)} & \text{Substrate region} \end{Bmatrix} \tag{A2}$$

where $k_C = \sqrt{\beta^2 - \varepsilon_C k_0^2}$, $k_A = \sqrt{\varepsilon_A k_0^2 - \beta^2}$, $k_F = \sqrt{\varepsilon_F k_0^2 - \beta^2}$, $k_M = \sqrt{\varepsilon_M k_0^2 - \beta^2}$ and $k_S = \sqrt{\beta^2 - \varepsilon_S k_0^2}$.

Also the dispersion relation for the proposed five layered waveguide

$$2\pi m = 2k_F d_F - \phi_{F,M,S} - \phi_{F,A,C} \tag{A3}$$

where
$$\phi_{F,M,S} = 2\tan^{-1}\left[i\left(\frac{1-r_{F,M}}{1+r_{F,M}}\right)\left(\frac{1-r_{M,S}e^{2ik_M d_M}}{1+r_{M,S}e^{2ik_M d_M}}\right)\right]$$
$$\phi_{F,A,C} = 2\tan^{-1}\left[i\left(\frac{1-r_{F,A}}{1+r_{F,A}}\right)\left(\frac{1-r_{A,C}e^{2ik_A d_A}}{1+r_{A,C}e^{2ik_A d_A}}\right)\right]$$
$$r_{F,M} = \frac{k_F - k_M}{k_F + k_M}, \quad r_{M,S} = \frac{k_M - k_S}{k_M + k_S},$$
$$r_{F,A} = \frac{k_F - k_A}{k_F + k_A}, \quad r_{A,C} = \frac{k_A - k_C}{k_A + k_C}$$

The reflectance of the proposed waveguide can be written as

$$R = |r_{S,M,F,A,C}|^2 = \left|\frac{r_{S,M} + r_{M,F,A,C}e^{2ik_M d_M}}{1 + r_{S,M}r_{M,F,A,C}e^{2ik_M d_M}}\right|^2 \tag{A4}$$

where

$$r_{M,F,A,C} = \frac{r_{M,F} + r_{F,A,C}\ e^{2ik_F d_F}}{1 + r_{M,F} r_{F,A,C}\ e^{2ik_F d_F}}, \quad r_{F,A,C} = \frac{r_{F,A} + r_{A,C}\ e^{2ik_A d_A}}{1 + r_{F,A} r_{A,C}\ e^{2ik_A d_A}}$$

$$r_{S,M} = \frac{k_S - k_M}{k_S + k_M}, \quad r_{M,F} = \frac{k_M - k_F}{k_M + k_F},$$

By matching the field at the boundaries we get a set of eight equations having eight unknown constants. These equations are written as

$$\Delta\psi = 0 \tag{A5}$$

where Δ is 8×8 determinant having elements given as follows

$$\begin{aligned}
a_{11} &= \exp(-k_S d_M);\ a_{12} = -\exp(-ik_M d_M);\ a_{13} = -\exp(ik_M d_M);\\
a_{14} &= 0;\ a_{15} = 0;\ a_{16} = 0;\ a_{17} = 0;\ a_{18} = 0;\ a_{21} = -k_S \exp(-k_S d_M);\\
a_{22} &= ik_M \exp(-ik_M d_M);\ a_{23} = -ik_M \exp(ik_M d_M);\ a_{24} = 0;\\
a_{25} &= 0;\ a_{26} = 0;\ a_{27} = 0;\ a_{28} = 0;\ a_{31} = 0;\ a_{32} = 1;\ a_{33} = 1;\\
a_{34} &= -1;\ a_{35} = -1; a_{36} = 0;\ a_{37} = 0;\ a_{38} = 0;\ a_{41} = 0;\ a_{42} = ik_M;\\
a_{43} &= -ik_M;\ a_{44} = -ik_F;\ a_{45} = ik_F;\ a_{46} = 0;\ a_{47} = 0;\ a_{48} = 0;\\
a_{51} &= 0;\ a_{52} = 0;\ a_{53} = 0;\ a_{54} = \exp(ik_F d_F);\ a_{55} = \exp(-ik_F d_F);\\
a_{56} &= -\exp(ik_A d_F);\ a_{57} = -\exp(-ik_A d_F);\ a_{58} = 0;\ a_{61} = 0;\\
a_{62} &= 0;\ a_{63} = 0;\ a_{64} = ik_F \exp(ik_F d_F);\ a_{65} = -ik_F \exp(-ik_F d_F);\\
a_{66} &= -ik_A \exp(ik_A d_F);\ a_{67} = ik_A \exp(-ik_A d_F);\ a_{68} = 0;\ a_{71} = 0;\\
a_{72} &= 0;\ a_{73} = 0;\ a_{74} = 0;\ a_{75} = 0;\ a_{76} = \exp(ik_A(d_A + d_F));\\
a_{77} &= -\exp(-ik_A(d_A + d_F));\ a_{78} = -\exp(-ik_C(d_A + d_F));\ a_{81} = 0;\\
a_{82} &= 0;\ a_{83} = 0;\ a_{84} = 0;\ a_{85} = 0;\ a_{86} = ik_A \exp(ik_A(d_A + d_F));\\
a_{87} &= -ik_A \exp(-ik_A(d_A + d_F));\ a_{88} = k_C \exp(-ik_C(d_A + d_F));
\end{aligned}$$

REFERENCES

1. Tiefenthaler, K. and W. Lukosz, "Integrated optical switches and glass sensor," *Opt. Letter*, Vol. 10, 137–139, 1984.
2. Tiefenthaler, K. and W. Lukosz, "Sensitivity of grating couplers as integrated optical chemical sensors," *Rev. Mod. Phys.*, Vol. 49, 361–420, 1977.
3. Kunz, R. E., "Miniature integrated optical modules for chemical and biological sensing," *Sens. Actuators B*, Vol. 38, 13–28, 1997.
4. Lukosz, W., "Integrated optical chemical and direct biochemical sensors," *Sens. Actuators B*, Vol. 29, 3750, 1995.

5. Horvath, R., G. Fricsovszky, and E. Pap, "Application of the optical waveguide lightmode spectroscopy to monitor lipid bilayer phase transition," *Biosensors Bioelectron.*, Vol. 18, 415–428, 2003.
6. Hervath, R., et al., "Optical waveguide sensor for on-line monitoring of bacteria," *Opt. Letter*, Vol. 28, 1233–1235, 2003.
7. Marazuela, M. D., et al., "Fiber-optic biosensors — An overview," *Anal. Bioanal Chem.*, Vol. 372, 664–682, 2002.
8. Ivnitski, D., et al., "Review: Biosensors for detection of pathogenic bacteria," *Biosens. Bioelectron*, Vol. 14, 599–624, 1999.
9. Udd, E., "An overview of fiber optic sensors," *Rev. Sci. Instrum.*, Vol. 66, 4015–4030, 1995.
10. Kuswandi, B., "Simple optical fiber biosensor based on immobilized enzyme for monitoring of trace having metal ions," *Anal. Bioanal. Chem.*, Vol. 376, 1104–1110, 2003.
11. Horvath, R., et al., "Measurement of guided light mode intensity: An alternative waveguide sensing principle," *Appl. Phys. Lett.*, Vol. 84, 4044–4046, 2004.
12. Homola, J., S. S. Yee, and G. Gauglitz, "Surface plasmon resonance sensors: Review," *Sensors and Actuators B*, Vol. 54, 3–15, 1999.
13. Sharma, A. K. and B. D. Gupta, "Theoretical model of a fiber optic remote sensor based on surface plasmon resonance for temperature detection," *Optical Fiber Technol.*, Vol. 12, 87–100, 2006.
14. Horvath, R., H. C. Pederson, and N. Skivensen, "Monitoring of living cell attachment and spreading using reverse symmetry waveguide sensing," *Appl. Phys. Letters*, Vol. 86, 071101–071103, 2005.
15. Skivensen, N., R. Horvath, and H. C. Pederson "Optimization of metal-clad waveguide sensor," *Sensor and Actuators B*, Vol. 106, 668–676, 2005.
16. Skivensen, N., R. Horvath, S. Thinggaaed, N. B. Larsen, and H. C. Pedersen, "Deep-probe metal-clad waveguide biosensors," *Biosensor and Bioelectronics*, Vol. 22, 1282–1288, 2007.
17. Ksendzov, A. and Y. Lin, "Integrated Optics ring-resonator sensor for protein detection," *Opt. Lett.*, Vol. 30, 3344–3346, 2005.
18. Yalcin, A., K. C. Popat, J. C. Aldridge, T. A. Desai, J. Hryniewicz, et al., "Optical sensing of biomolecules using micro -ring resonators," *IEEE J. Sel. Topics Quantum Electron*, Vol. 12, 148–154, 2006.
19. Blanco, F. J., M. Agirregabiria, J. Berganzo, K. Mayora,

J. Elizalde, et al., "Microfluidic optical Integrated CMOS compatible devices for level free biochemical sensing," *J. Micromech. Microeng.*, Vol. 16, 1006–1016, 2006.

20. Densmore, A., D. X. Xu, P. Waldron, S. Janz, P. Cheben, J. Lapointe, et al., "A silicon-on-insulator photonic wire based evanescent field sensor," *IEEE Photonics Technology Letters*, Vol. 18, No. 23, 2520–2522, 2006.
21. Veldhuis, G. J., O. Parriaux, H. J. W. Hockstra, and P. V. Lambeck, "Sensitivity enhancement in evanescent optical waveguide sensors," *J. of Lightw. Technol.*, Vol. 18, 677–682, 2000.
22. Jourab, M., et al., "The development of a metal clad waveguide sensor for the detection of particles," *Sensors and Actuators B*, Vol. 90, 296–307, 2003.
23. Jourab, M., et al., "An integrated metal clad leaky waveguide sensor for detection of bacteria," *Anal. Chemistry*, Vol. 77, 232–242, 2005.
24. Taya, S. A., M. M. Shabat, and H. M. Khalil, "Enhancement of sensitivity in optical waveguide sensors using left-handed materials," doi:10.1016/j.ijleo.2007.12.001, 2007.
25. Huang, S. Y. and S. Y. Wang, "Light propagation characteristics in various dielectric waveguide," *Chinese Journal of Physics*, Vol. 24, No. 2, 129–137, 1986.
26. Fletchert, M. and G. I. Loeb, "Influence of substratum characteristics on the attachment of a marine pseudomonad to solid surfaces," *Applied and Environmental Microbiology*, Vol. 37, No. 1, 67–72, 1979.
27. Morell, A. and Y. H. Ahn, "Optical efficiency factors of free-living marine bacteria: Influence of bacterioplankton upon the optical properties and particulate organic carbon in oceanic waters," *Journal of Marine Research*, Vol. 48, 145–175, 1990.
28. Lavers, C. R., K. Itoh, S. C. Wu, M. Murabayashi, I. Mauchline, G. Stewart, and T. Stout, "Planar optical waveguides for sensing applications," *Sensors and Actuators B*, Vol. 69, 85–95, 2000.
29. Campbell, A. N., E. M. Kartzmark, and W. E. Falconer, "The system: Nicotine-methylethyl ketone-water," *Can. J. Chem.*, Vol. 36, 1475–1486, 1958.
30. Debenham, M. and G. D. Dew, "The refractive index of toluene in the visible spectral region," *J. Phys. E: Sci. Instrum.*, Vol. 14, 544–545, 1981.
31. Rostami, A. and H. Motavali, "Asymptotic iteration method: A powerful approach for analysis of inhomogeneous dielectric slab

waveguides," *Progress In Electromagnetics Research B*, Vol. 4, 171–182, 2008.

32. Wang, Z. J. and J. F. Dong, "Analysis of guided modes in asymmetric left-handed slab waveguides," *Progress In Electromagnetics Research*, PIER 62, 203–215, 2006.
33. Liu, S.-H., C.-H. Liang, W. Ding, L. Chen, and W.-T. Pan, "Electromagnetic wave propagation through a slab waveguide of uniaxially anisotropic dispersive metamaterial," *Progress In Electromagnetics Research*, PIER 76, 467–475, 2007.